AIR-SOURCE HEAT PUMP PERFORMANCE COMPARISON IN DIFFERENT REAL OPERATIONAL CONDITIONS BASED ON ADVANCED EXERGY AND EXERGOECONOMIC APPROACH

by

Goran D. VUČKOVIĆ*, Mirko M. STOJILJKOVIĆ, Marko G. IGNJATOVIĆ, and Mića V. VUKIĆ

Faculty of Mechanical Engineering, University of Nis, Nis, Serbia

Original scientific paper
https://doi.org/10.2298/TSCI200529237V

The use of air-source heat pumps (ASHP) is increasing to meet the energy needs of residential buildings, and manufacturers of equipment have permanently expanded the range of work and improved the efficiency in very adverse outdoor air conditions. However, in the time of a wide range of different technologies, the problem of using ASHP, from a techno-economic point of view, is constantly present. Exergetic efficiency and exergoeconomic cost no longer provide sufficiently reliable information when it is necessary to reduce the investment costs or increase the energy/exergetic efficiency of the component/system. This paper presents comparison of ASHP in different operational conditions based on an advanced exergy and exergoeconomic approach. The advanced exergy analysis splits the destruction of exergy for each individual component into avoidable and unavoidable part in order to fully understand the processes. The information of stream costs is used to calculate exergoeconomic variables associated with each system component. Irreversibility in the compressor have the greatest impact on reducing the overall system exergetic efficiency by 46.7% during underfloor heating (UFH) operation and 24.53% during domestic hot water (DHW) operation. Exergy loss reduces exergetic efficiency by 5.72% UFH and 39.74% DHW. High values of exergoeconomic cost for both operating regimes are present in flows 1, 2, 3 and 4 due to high costs of production and relatively small exergy levels. The general recommendation is to set the ASHP to operate with near-optimal capacities in both regimes and then reduce exergy of flows 1, 2, 5, 11, and 13.

Keywords*: exergy, exergoeconomic, heat pump, UFH, DHW.*

Introduction and background

The building sector has become the largest consumer of primary energy in the world, exceeding both the industry and the transportation sectors. Heat pump technology can deliver major economic, environmental and energy system benefits worldwide. The technology is now becoming one of the corner stones of the energy mix for decarbonising heating and cooling in industry, the building sector and society at large. Most heat pump systems in common use today are of the vapour-compression type [1].

* Corresponding author, e-mail: goran.vuckovic@masfak.ni.ac.rs

Considering the heat source of a heat pump, there are three basic types: ASHP, water-source heat pump (WSHP), and ground-source heat pump (GSHP). Yet, in order to fully define and analyse heat pump operation, information on the heat sink is also needed. For heat pumps, usually water or air are used as heat sinks. Concurrently, each of the above three heat pump types has two subtypes, *i.e.* air-source-air-sink heat pump or air-source-water-sink heat pump (ASWSHP). For this paper the following terms and abbreviations are used: air-to-air heat pump (AAHP), air-to-water heat pump (AWHP), water-to-air heat pump, water-to-water heat pump, ground-to-air heat pump, and ground-to-water heat pump.

More than 18 million households worldwide purchased heat pumps in 2018, up from 14 million in 2010. Nearly 80% of new household heat pump installations in 2017 were in China, Japan, and the USA, which together account for around 35% of the global final energy demand for space and water heating in residential buildings. Air source heat pumps, especially AAHP, dominate global sales for space heating in the building sector. Also, other subtypes of ASHP, such as AWHP, and both types of WSHP and GSHP, have also expanded in recent years. In Japan, Korea, Europe, and USA, reversible heat pumps are commonly used for heating and cooling, which often means higher heat pump performance. The adjustment of the refrigerant flow rate reduces energy losses resulting from stops and starts in non-inverter technologies [2].

The European Heat Pump Association statistics for 2018 reports more than 1.2 million heat pumps (+12%) sold in Europe, leading to an installed capacity of 11.8 million units. This installed stock contributed 29.8 Mt of carbon emission reduction and 116 TWh of energy generated from renewable sources. It helped reduce the final energy demand by 148 TWh and ensured a total of 54000 full time equivalent jobs in Europe. If properly connected, the current stock of heat pumps could provide the demand side flexibility between 1 and 3.2 TWh over the course of a year. Splitting up the overall sales development in Europe by *energy source used* reveals the dominance of ASHP in the market [3].

Simple installation, very good performances related to low temperature systems operated in mild outside conditions (> –6 °C), low investment and maintenance costs are the main advantages of ASHP. However, during extremely low outside temperatures, if high supply water temperatures for heating and/or DHW preparation (>45 ^{o}C) are required, and during intermittent operation with high frequency of intermittence, ASHP efficiency decreases significantly. This leads to increased power consumption and consequently to increased GHG emissions and operation costs. Selection of working fluid, adjustability to electricity tariff system, reducing heat losses, high efficiency over large span of operation temperatures are permanent tasks for the research community and heat pump industry.

The objective of paper [4] is to demonstrate the application and usefulness of advanced exergy analysis to the evaluation of vapour compression refrigeration machines when different one-component working fluids (R125, R134a, R22, and R717) as well as azeotropic (R500) and zeotropic (R407C) mixtures are used, and to study the effect of different material properties on the results of advanced exergy analysis. The advantages of an advanced exergy analysis become more transparent and evident when an advanced exergoeconomic evaluation is conducted, particularly for complex systems.

Dong *et al*. [5] proposes and investigates the solar integrated air source heat pump (SIASHP) with working fluid R407C for radiant floor heating without water. The SIASHP for radiant floor heating without a water pipe exposed to the outdoor environment is safe and convenient for the narrow and vertical outdoor installation space of high-rise building users to meet their individual demand for space heating.

The aim of paper [6] is to develop a more physics-based model to simulate the energy performance of variable refrigerant flow (VRF) heat recovery systems. The model categorizes the operations of the VRF heat recovery system into six modes based on the indoor cooling/heating requirements and the outdoor unit operational states and uses novel algorithms to capture the control logic and heat recovery between indoor units. The work presented in this paper introduces the development, implementation, and validation of the new model. Results show that the new model can present a satisfactory match with the measured data across all the operation modes at sub-hourly levels.

Qui *et al*. [7] present an energy performance evaluation of a low global warming potential refrigerant, L-41b, as a replacement for R410A. The experiment was carried out in the climatic chamber, where the temperature was maintained within a range between 10 °C and 30 °C. The condenser outlet water temperature was controlled between 25 °C and 45 °C, followed by maintaining the water temperature difference of 5 °C in the condenser inlet and outlet. Adopting an internal heat exchanger has the potential of lowering the differences of performance, besides approaching the L-41b performance to that attained with the use of R410A in the existing ASHP. The refrigerant R410A is used a lot in vapour compression refrigeration and air conditioning systems due to its high energy efficiency ratio [8].

The application of ASHP is mainly restricted by the outdoor ambient temperature, which causes poor application effects in the severe cold regions of China. Xu *et al*. [9] proposes an innovative hybrid energy system of a solar air collector, ASHP and energy storage that is utilized to save energy for ultra-low energy building in severe cold regions. The results indicate that, where the outdoor heating calculation temperature is lower than –30 °C and solar energy resources are not particularly abundant, the peak inlet air temperature of the ASHP increases by no less than 10 °C and the coefficient of performance of the system is expected to be higher than 3.0 under extremely low temperature conditions.

Ahamed *et al*. [10] reviews the possibilities of research in the field of exergy analysis in various usable sectors where vapour compression refrigeration systems are used. It is found that exergy depends on evaporating temperature, condensing temperature, sub-cooling, and compressor pressure. Exergy losses increase with the increase in suction and discharge temperature of the compressor. For better performance of the system, compressor discharge and suction temperature should be within 65 °C and 14 °C, respectively.

The aim of paper [11] is to investigate the feasibility of using ground source heat pump systems in hot and dry regions. This paper introduces for the first time a techno-economic analysis to evaluate the use of GSHP compared to the conventional ASHP in this type of climate, in the example of Saudi Arabia. It is concluded that the GSHP is feasible, albeit with a long payback period, typically 10-20 years, depending on the conditions, set-up, and predictions.

Wang *et al*. [12] presents the energy and exergy analysis of an ASHP water heater system using CO_2/R170 mixture as an azeotropy refrigerant for sustainable development. For a CO_2/R170 ASHP water heater system, it is more important to choose a proper capillary tube as throttling device to obtain better exergy efficiency than the one for an R134a system.

Byme and Ghoubali [13] presents the evolution of an exergy analysis of ASHP for simultaneous production of heating and cooling energies for residential buildings, hotels, or office buildings. The experimental results show that the R290 (propane) has a higher performance than R407C regarding exergy aspects thanks to not only the refrigerant choice but also to a better design of components.

Su *et al*. [14] provides detailed energy, exergy and exergoeconomic analyses performed for a frost-free air-conditioning system with integrated liquid desiccant dehumidification and compressor-assisted regeneration, in which the diluted liquid desiccant can be efficiently regenerated under low temperature conditions. When the proposed system is optimized based on the exergoeconomics, the coefficient of performance and exergy efficiency increase by 13.02% and 12.73%, respectively. The total product unit costs can decrease by 12.64% compared to that under the basic operation condition.

This paper analyses a vapour compression ASWSHP, or AWHP for short, in real operating conditions. For measured operation parameters, advanced exergy analysis and exergoeconomic evaluation is applied in order to identify real losses and to quantify the possibilities for improving operating efficiency. Having in mind that heat pumps are used in residential buildings, mainly for both space heating and DHW preparation, two different operating modes are analysed: the heat pump operates in a low temperature mode for space heating through the UFH system and the heat pump operates in a high temperature mode for DHW preparation.

Description of AWHP and processes of water heating

A schematic of a vapour compression AWHP is shown in fig. 1. The heat pump system consists of two separate circuits: heat pump circuit (refrigerant/primary circuit) and heat distribution circuit (water/secondary circuit). The refrigerant or heat transfer fluid is R410A. The heat pump is constructed as a split-system with an outdoor and an indoor unit, connected with copper piping for vapour and liquid phases of the refrigerant. The outdoor unit consists of a compressor (CM), an evaporator (EV) with a fan (FA), a four-way/reversing valve (RV), and a throttling valve (TV). The indoor unit is conceived as an integral free-standing unit with two subsystems: hydro-module and DHW tank. The hydro-module consists of a plate heat exchanger/condenser (CD), a three-way/diversion valve (DV), and a circulating pump (CP). The DHW tank is conceived as a vertical accumulation-type tank with the total volume of 180 L, with a spiral heat exchanger placed in the lower zone of the tank. The accumulation tank is factory pre-insulated in order to minimize heat losses.

The heat pump operates in the heating mode, so reversing the valve position enables the refrigeration cycle, fig. 1. In the vapour compressor, equipped with an inverter drive (inverter type), slightly overheated low-pressure vapour (state 1) is compressed to a higher pressure and temperature, which is registered with digital sensors. Superheated high pressure vapour (state 2) enters the condenser where it condenses and slightly cools down (state 3). The temperature is measured in this point. Reducing liquid pressure is done in the throttling valve (isenthalpic). The cold liquid-vapour mixture (state 4) enters the evaporator where it evaporates by cooling the surrounding air, heat source, figs. 1(a) and 1(b), and is slightly overheated (state 1). The evaporation temperature is measured with a surface mounted temperature sensor. Heat transfer in the evaporator is intensified by continuous operation of a frequency driven axial fan. In order to maximize heat transfer from the surrounding air, during the heating operation, the axial fan operates at full capacity. Cooled, the surrounding air leaves the evaporator in state 12.

Circulating water from the secondary circuit (used for space heating and/or DHW preparation) is used as a heat sink. This water is heated in the condenser of the heat pump. The condenser is constructed as a highly efficient counterflow plate heat exchanger, additionally insulated in order to minimize heat losses. Circulating water flow and temperature (state 6) are measured at the condenser inlet and additionally leaving water temperature is measured at the condenser outlet, state 7(8). The circulating pump is also frequency driven.

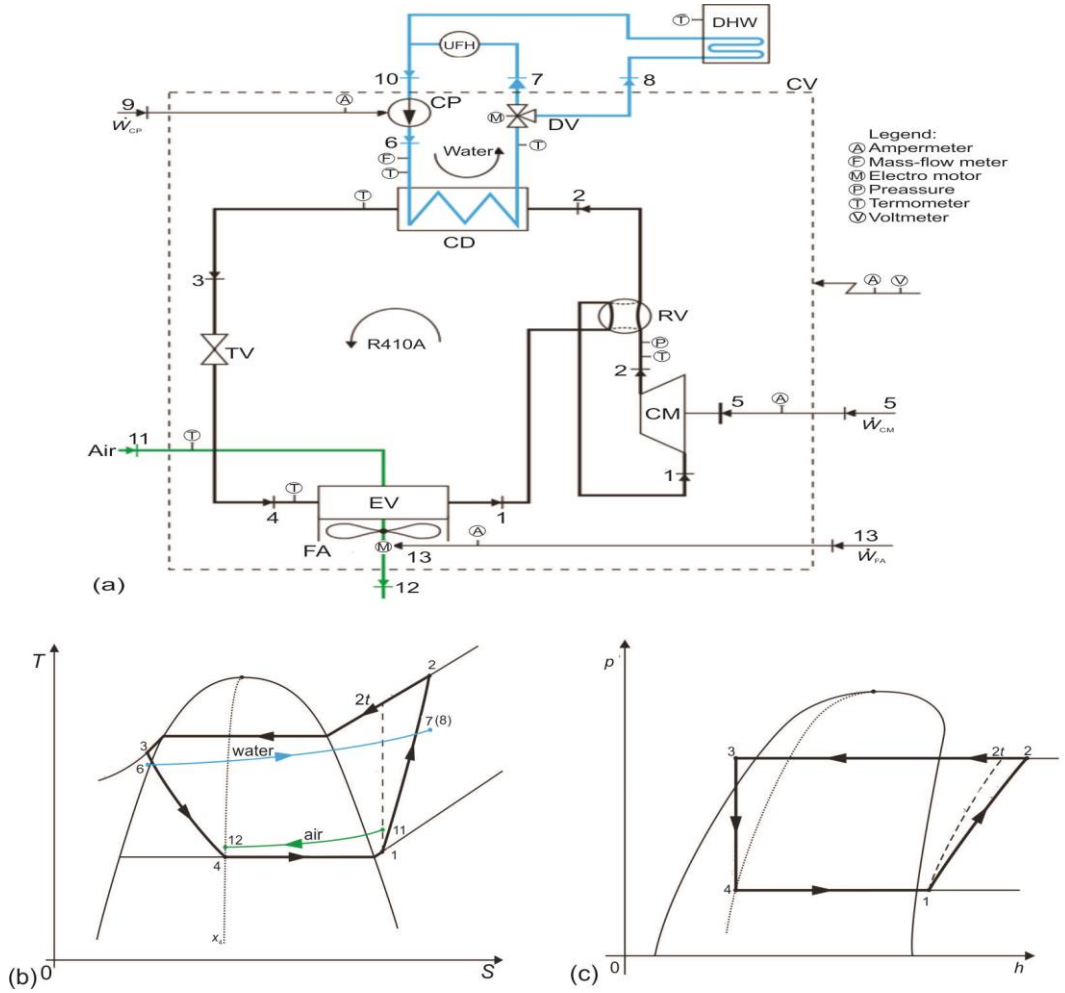

Figure 1. Flow diagram of AWHP and respective diagrams of the vapour-compression cycle; (a) flow diagram of AWHP with positions of measuring equipment, (b) temperature-entropy diagram, and (c) pressure-enthalpy diagram (log*p*-*h*)

The supply of electricity to the compressor, the axial fan and the circulating pump is managed through a 230V AC power supply, and represented with energy flows 5, 9, and 13. Electricity is provided by an official distributor. For all three components the electric current is measured with ammeters, fig. 1(a).

For the purpose of this research, two different heating energy consumers are analysed: UFH of space at low temperature ($t_7 = t_{UFH,sp} = 38$ °C) and DHW preparation in an accumulation tank at higher temperature levels ($t_{DHW,sp} = 46$ °C). Heating energy supply changeover is done with an electrically actuated three-way valve, fig. 1(a). When the valve is in Position I, space heating is enabled (cycle, 7-10-6), while when it is in Position II DHW preparation is running (cycle 8-10-6). In total, 13 spot measurements are performed (7 for temperature readings, 4 for electricity, 1 for water flow, and 1 for pressure).

The heat pump was used for space heating in the period from 00:14:50 to 02:09:40 (30-01-2020), during which 690 readings were recorded for every measuring spot, resulting in

a total of 8970 readings. During this operation the control parameter was the supply water temperature with a set point of 38 °C ($t_7 = t_{UFH,sp}$ = 38 °C). The set point was reached in 8 minutes and 30 seconds, and after this point the heat pump was in the modulating regime, *i.e.* the compressor and the circulating pump were adjusted to real demand. Since starting with the modulating regime, the heat pump (set point was) reached (full control) after 55 minutes and 20 seconds, fig. 2(a). The DHW preparation ran in the period from 22:15:20 to 22:48:00 (29-01-2020), during which 197 readings were recorded per measuring spot, resulting in a total of 2561 readings. In this case, the control parameter was the tank water temperature with a set point of 46°C ($t_{DHW,sp}$ = 46 °C). The set point was reached in 36 minutes and 40 seconds, resulting in the unit being switched off, fig. 2(b). The ASHP operation was monitored and the parameters were recorded with the measuring equipment supplied by producer (for temperature thermistors with negative temperature coefficient and interchange ability ± 0.1 °C).

Methodology and modelling

When we think about energy, we consider it in terms of quantity. However, in a resource-constrained world, energy must also be appreciated from the point of view of quality, which is essentially a measure of its usefulness, or its ability to do work. In order to account for the quality and not just the quantity of energy, we need to measure exergy. The exergy approach can identify and quantify the causes of internal inefficiencies. Exergy is the right metric to value energy, use and resource scarcity [15].

Mass, energy, entropy, and exergy balances are employed to determine the heat transfer, the entropy generation rate or the rate of exergy destruction. The mass, energy, entropy, and exergy balance equations for a component k of an energy system in the steady-state conditions have the form, respectively [16]:

$$0 = \sum_i \left(\dot{m}_i\right)_k - \sum_e \left(\dot{m}_e\right)_k \tag{1}$$

$$0 = \dot{Q}_{\mathrm{cv},k} - \dot{W}_{\mathrm{cv},k} + \sum_i \left(\dot{m}_i h_i\right)_k - \sum_e \left(\dot{m}_e h_e\right)_k \tag{2}$$

$$0 = \sum_j \left(\frac{\dot{Q}_j}{T_j}\right)_k + \sum_i \left(\dot{m}_i s_i\right)_k - \sum_e \left(\dot{m}_e s_e\right)_k + \dot{S}_{\mathrm{gen},k} \tag{3}$$

$$0 = \sum_j \left[\left(1 - \frac{T_0}{T_j}\right)\dot{Q}_j\right]_k - \dot{W}_{\mathrm{cv},k} + \sum_i \left(\dot{m}_i e_i\right)_k - \sum_e \left(\dot{m}_e e_e\right)_k - \dot{E}_{\mathrm{D},k} \tag{4}$$

The total exergy of a material stream consists of four exergy components: physical, chemical, kinetic, and potential. For this paper, the physical exergy is more interesting. The physical exergy of a stream of matter can be defined as the maximum work (useful energy) that can be obtained from it when taking it to the physical equilibrium (of temperature and pressure) with the environment. For calculating exergy-related parameters, standard conditions for temperature and pressure were applied, *i.e.* T_0 = 298.15 K, p_0 = 1.01325 bar. The specific physical exergy transfer associated with a stream of matter is:

$$e_j^{\mathrm{PH}} = e_j = \left(h_j - h_0\right) - T_0\left(s_j - s_0\right) \tag{5}$$

The last term on the right-hand side of eq. (4) represents the exergy destruction of the k^{th} component of the system. Exergy destruction is proportional to generated entropy, with the surrounding temperature being the constant of proportionality. This equation is known in the literature as the theorem of the loss of capability to do work, exergy destruction theorem or Gouy-Stodola theorem. For the known value of the generated entropy for the k^{th} component of an energy system, obtained from entropy balance (3), exergy destruction is obtained as [16]:

$$\dot{E}_{\mathrm{D},k} = T_0 \dot{S}_{\mathrm{gen},k} \tag{6}$$

Exergy destruction in the overall system is obtained by summing up exergy destruction of every component of the system:

$$\dot{E}_{\mathrm{D},tot} = \sum_{k=1}^{n} \dot{E}_{\mathrm{D},k} \tag{7}$$

Energy transfer *i.e.* heat transfer is followed by entropy transfer, while work transfer is performed without entropy transfer. While obtaining work from supplied heat, the general idea is to obtain as much as possible useful work, having in mind that heat removed to a heat sink is not a loss, but necessary compensation to obtain useful work from heat. In the case of a heat pump, maximum efficiency is reached when heat pumps operate in the ideal Carnot cycle with reversible processes (isentropic and isothermal processes), with efficiency dependent only on heat source temperature (evaporation temperature) and heat sink temperature (condensing temperature) [17]:

$$COP_{\mathrm{C}} = \frac{T_{\mathrm{con}}}{T_{\mathrm{con}} - T_{\mathrm{evp}}} \tag{8}$$

All real thermodynamic cycles have efficiency lower than the Carnot cycle situated between the highest and the lowest temperature of a real cycle. The energy-based efficiency measure (COP) of the overall heat pump system under consideration in this paper can be defined as:

$$COP_{\mathrm{tot}} = \frac{\dot{Q}_{\mathrm{EU}}}{\dot{W}_{\mathrm{tot}}}, \quad \left(COP_{\mathrm{tot}} < COP_{\mathrm{C}}\right) \tag{9}$$

The dividend in eq. (9) represents the heat delivered to the end-user, in the first case it is the heat delivered to the space heating system, $\dot{Q}_{EU} = \dot{Q}_{UFH} = \dot{m}_w \left(h_7 - h_{10}\right)$, and in the second case the heat delivered to the DHW preparation system, $\dot{Q}_{\mathrm{EU}} = \dot{Q}_{\mathrm{DHW}} = \dot{m}_w \left(h_8 - h_{10}\right)$.

True information on a system's energy performance, in the sense of thermodynamic characteristics, is the efficiency based on exergy, *i.e.* exergetic (2^{nd} Law) efficiency. In the fuel-product concept, exergetic efficiency is defined as the ratio between exergy of products and fuel (component/overall system) [18]:

$$\varepsilon_k = \frac{\dot{E}_{\mathrm{P},k}}{\dot{E}_{\mathrm{F},k}} = 1 - \frac{\dot{E}_{\mathrm{D},k} + \dot{E}_{\mathrm{L},k}}{\dot{E}_{\mathrm{F},k}}, \quad \varepsilon_{\mathrm{tot}} = \frac{\dot{E}_{\mathrm{P,tot}}}{\dot{E}_{\mathrm{F,tot}}} = 1 - \frac{\dot{E}_{\mathrm{D,tot}} + \dot{E}_{\mathrm{L,tot}}}{\dot{E}_{\mathrm{F,tot}}} \tag{10}$$

For a proper determination of exergy efficiency, it is of crucial importance to properly define exergy of fuel and exergies of the products for every component of the system

and the overall system [16]. The definitions of fuel and product exergies for all components and the overall system are given in tab. 1. In the fuel-product concept, for the steady-state, component and system exergy balance is given by equations:

$$\dot{E}_{\mathrm{F},k} = \dot{E}_{\mathrm{P},k} + \dot{E}_{\mathrm{D},k} + \dot{E}_{\mathrm{L},k}, \quad \dot{E}_{\mathrm{F,tot}} = \dot{E}_{\mathrm{P,tot}} + \dot{E}_{\mathrm{D,tot}} + \dot{E}_{\mathrm{L,tot}} \tag{11}$$

For eqs. (10) and (11) it should be stated that when the component boundary is set at the surrounding temperature (most often the case), the exergy loss has a zero value ($\dot{E}_{\mathrm{L},k} = 0$), *i.e.* the complete loss of work of the component can be attributed to its exergy destruction, while the exergy loss of the whole system remains ($\dot{E}_{\mathrm{L},tot} \neq 0$). In order to determine the influence of the exergy loss of every component and the overall system on the system's exergetic efficiency, in this research the coefficients of exergy destruction for the component and the system were determined with the following equations [16]:

$$y_{\mathrm{D},k} = \frac{\dot{E}_{\mathrm{D},k}}{\dot{E}_{\mathrm{F,tot}}}, \quad y_{\mathrm{L,tot}} = \frac{\dot{E}_{\mathrm{L,tot}}}{\dot{E}_{\mathrm{F,tot}}} \tag{12}$$

When these coefficients (12) are transformed to percentages, one can determine the percentage of influence of each component on the system's exergetic efficiency.

In order to prioritize components for performance improvements, it is good to quantify the share of a component's exergy destruction in the total exergy destruction of the system. This is done by determining the coefficient of the total exergy destruction of component k [18]:

$$y^{*}_{\mathrm{D},k} = \frac{\dot{E}_{\mathrm{D},k}}{\dot{E}_{\mathrm{D,tot}}} \tag{13}$$

Within advanced exergy analysis, the total exergy destruction of a component determined by means of conventional exergy analysis is separated into the unavoidable and avoidable part, $\dot{E}_{\mathrm{D},k} = \dot{E}^{\mathrm{UN}}_{\mathrm{D},k} + \dot{E}^{\mathrm{AV}}_{\mathrm{D},k}$. For determining the unavoidable part of exergy destruction, for a component of the system, unavoidable operating conditions were pre-defined, tab. 1., as such operating conditions cannot be reached quickly, having in mind the current technology progress. Every component was analysed independently from the other components of the system, and for unavoidable operating conditions, the specific unavoidable exergy destruction was defined as: $\left(\dot{E}_{\mathrm{D},k}/\dot{E}_{\mathrm{P},k}\right)^{\mathrm{UN}}$. The unavoidable and avoidable parts of exergy destruction of component k were determined, respectively, as [19]:

$$\dot{E}^{\mathrm{UN}}_{\mathrm{D},k} = \dot{E}_{\mathrm{P},k}\left(\frac{\dot{E}_{\mathrm{D},k}}{\dot{E}_{\mathrm{P},k}}\right)^{\mathrm{UN}} \tag{14}$$

$$\dot{E}^{\mathrm{AV}}_{\mathrm{D},k} = \dot{E}_{\mathrm{D},k} - \dot{E}^{\mathrm{UN}}_{\mathrm{D},k} \tag{15}$$

The avoidable part (15) represents the real potential for component improvement. Based on advanced exergy analysis, the maximum exergetic efficiency for every component of the system was determined as [20]:

$$\varepsilon_k^{\max} = \frac{1}{1+\left(\frac{\dot{E}_{\mathrm{D},k}}{\dot{E}_{\mathrm{P},k}}\right)^{\mathrm{UN}}} \tag{16}$$

Every component will have maximum exergy efficiency when it operates with minimum specific unavoidable exergy destruction, the term in the brackets in eq. (16).

The scientific community is unanimous in claims that exergy is the proper thermodynamic characteristic to correspond with economic principles. In this sense, for the purpose of this research, the following exergoeconomic variables were used: exergoeconomic cost for electricity and energy flows, exergoeconomic cost for exergy destruction and relative cost analysis.

For determining exergoeconomic costs it is necessary to create an exergoeconomic balance for every component of the system. The exergoeconomic balance for a component shows that the sum of exergoeconomic costs for electricity and heat flows leaving the component is equal to the sum of exergoeconomic costs for electricity and heat flows entering the component and non-exergy related costs for capital investment and maintenance and operation costs, and is given in the form [16]:

$$\sum_e \left(c_e \dot{E}_e\right)_k + c_{\mathrm{w},k}\dot{W}_k = c_{\mathrm{q},k}\dot{E}_{\mathrm{q},k} + \sum_i \left(c_i \dot{E}_i\right)_k + \dot{Z}_k^{\mathrm{CI}} + \dot{Z}_k^{\mathrm{OM}} \tag{17}$$

Quantities related to exergy are determined by exergy analysis, while quantities for non-exergy related costs are determined as levelized annual costs for capital investment, operation, and maintenance costs per unit of time (year, hour, second). Since this research analysed the existing system in real operating conditions, capital investment costs were neglected.

Exergoeconomic costs basically represent money costs of energy and material flows. In the fuel-product concept, the component's (system's) exergoeconomic cost balance, for steady-state conditions, was defined in form [20]:

$$\dot{C}_{\mathrm{P,k}} = \dot{C}_{\mathrm{F,k}} + \dot{Z}_{\mathrm{k}}^{\mathrm{CI}} + \dot{Z}_{\mathrm{k}}^{\mathrm{OM}}, \quad \dot{C}_{\mathrm{P,tot}} = \dot{C}_{\mathrm{F,tot}} + \dot{Z}_{\mathrm{tot}}^{\mathrm{CI}} + \dot{Z}_{\mathrm{tot}}^{\mathrm{OM}} \tag{18}$$

According to the previous eq. (18), for a single component and for the overall system, for steady-state conditions, exergoeconomic cost of products equals the sum of exergoeconomic costs for resources and non-exergy related costs for capital investment, maintenance, and operation.

Exergoeconomic cost of exergy destruction represents the cost of fuel additionally provided to a single component/the overall system, in order to offset the disturbance caused by exergy destruction within the component/system. It is determined as the product of specific exergoeconomic fuel cost and exergy destruction of the given component/system [18]:

$$\dot{C}_{\mathrm{D},k} = c_{\mathrm{F},k}\dot{E}_{\mathrm{D},k} \quad \left(\dot{E}_{\mathrm{P},k} = \mathrm{const.}\right), \quad \dot{C}_{\mathrm{D,tot}} = c_{\mathrm{F,tot}}\dot{E}_{\mathrm{D,tot}} \quad \left(\dot{E}_{\mathrm{P,tot}} = \mathrm{const.}\right) \tag{19}$$

Relative cost differences as an exergoeconomic variable, representing a relative increase in average costs per unit of exergy, between fuel and product for the component/system was determined according [16]:

$$r_k = \frac{c_{\mathrm{P},k} - c_{\mathrm{F},k}}{c_{\mathrm{F},k}}, \quad r_{\mathrm{tot}} = \frac{c_{\mathrm{P,tot}} - c_{\mathrm{F,tot}}}{c_{\mathrm{F,tot}}} \tag{20}$$

It is desirable that the value of the relative cost analysis is as low as possible.

Results and discussions

The results presented in this paper are related to a low temperature AWHP with the nominal capacity of the outdoor unit of 6 kW and a single-phase electricity connection (model ERLQ006CV3) and the indoor unit with an integrated hydro-module and a 180 L. The DHW tank (model EHVX08S18CB3V).

Table 1 gives the overview of equations for calculating exergy of fuels, exergy of products, as well as real and unavoidable operating conditions for splitting exergy destruction into the avoidable and unavoidable part, for a single component and the overall system.

Table 1. Exergy of fuel, exergy of product, real and unavoidable operational conditions (OC) for components and system

Component	Exergy of fuel	Exergy of product	Real OC	Unavoidable OC
Compressor	$\dot{W}_{CM}$	$\dot{E}_2 - \dot{E}_1$	$\eta < 0.85$; $\dot{Q}_L \neq 0$	$\eta = 0.95$; $\dot{Q}_L \approx 0$
Condenser	$\dot{E}_2 - \dot{E}_3$	$\dot{E}_{7(8)} - \dot{E}_6$	$\Delta p' = 0$; $\Delta p'' \neq 0$; $\dot{Q}_L \neq 0$	$\Delta p' = 0$; $\Delta p'' \approx 0$; $\dot{Q}_L \approx 0$
Throttling valve	$\dot{E}_3$	$\dot{E}_4$	h = const.; $\dot{Q}_L \neq 0$	h = const.; $\dot{Q}_L \approx 0$
Evaporator	$\dot{W}_{FA} + (\dot{E}_{12} - \dot{E}_{11})$	$\dot{E}_4 - \dot{E}_1$	$\Delta p' = \Delta p'' = 0$; $\dot{Q}_L \neq 0$	$\Delta p' = \Delta p'' = 0$; $\dot{Q}_L \approx 0$
Circulation pump	$\dot{W}_{CP}$	$\dot{E}_6 - \dot{E}_{10}$	$\eta = 0.80$	$\eta = 0.95$
Heat pump	$\dot{W}_{tot} + (\dot{E}_{12} - \dot{E}_{11})$	$\dot{E}_{7(8)} - \dot{E}_{10}$	–	–

A comparison of AWHP performance in real operating conditions is done for two distinctive regimes.

During UHF operation, fig. 2(a)., the objective was to reach the space heating system supply water temperature of 38 °C ($t_7 = t_{UFH,sp}$ = 38 °C). During start-up, this temperature was 35.7 °C. The heat pump compressor started at full capacity leading to a permanent temperature rise of vapour at the compressor outlet from 54.5 °C to the maximum of 93.0 °C. Condensing temperature was increased in this period from 38.1 °C to the maximum of 44.6 °C. Supply water temperature was reached in 8.5 minutes. The set-point was exceeded due to the system's inertia, and this triggered the modulating operation of the heat pump, *i.e.* the compressor power supply was changed according to the actual heat demand.

The modulating operation led to a decrease in heat capacity (at first vapour temperature at the compressor outlet was steadily decreasing, leading to a condensing temperature decrease, and later to a further decrease in temperature variations), and after 55.5 minutes, the heat pump reached full control, with temperature set-point deviations smaller than ±0.4 °C, *i.e.* ≤ 1.0%. Vapour temperature at the compressor outlet was steadily around 60 °C. Heat source (outdoor air, t_{11}) temperature during the same time was in the range from 5.0 °C to –0.5 °C and it was followed by evaporating temperature and, since from eq. (8) it is desirable to have a smaller difference between condensing and evaporating temperature, led to the heat pump performance increase ($\Delta t_{lift}\downarrow \Rightarrow COP_C\uparrow$).

During DHW preparation, fig. 2(b)., the objective was to reach DHW tank temperature $t_{DHW,sp}$ = 46 °C, and during this operation the tank was treated as the end-user. At the beginning of operation, DHW tank temperature was 34.2 °C (this value can be treated as the *ghost* value due to the sensor position and stationary conditions), and immediately after the start it dropped to 29.9 °C after 7 minutes of operation (this temperature represents the actual, real temperature for the analysis). The heat pump compressor started at full capacity leading to a permanent temperature rise of vapour at the compressor outlet from 64.5 °C to the maximum of 96.5 °C, and after certain time this temperature was steadily around 90 °C. Condensing temperature increased from 37.0 °C to the maximum of 56.9 °C.

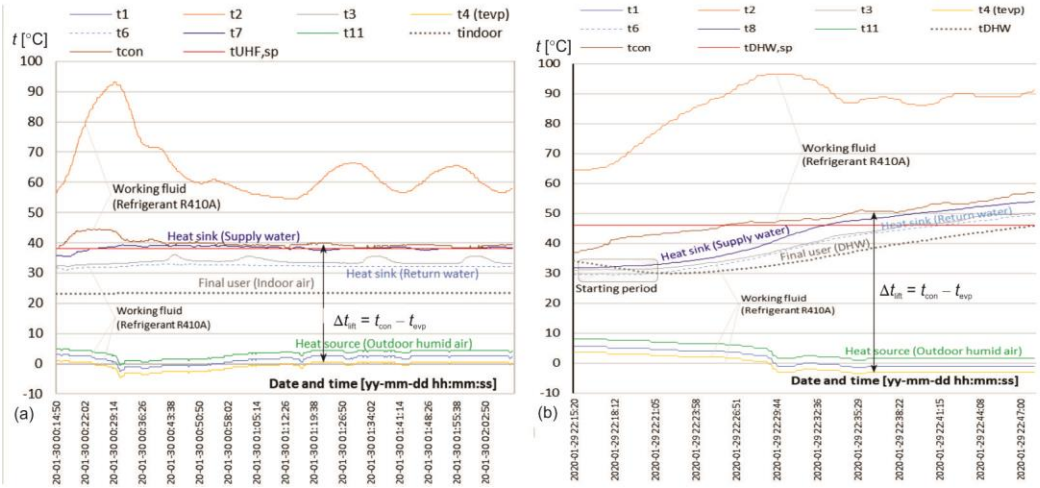

Figure 2. Temperature profiles of process fluids during real operating conditions; (a) low temperature UFH and (b) DHW heating

During the same time, heat source temperature (outdoor air, t_{11}) was between 1.0 °C and 8.0 °C, and it was followed by evaporating temperature. Unlike UHF operation, in this situation the heat pump did not enter the modulating operation since it shut down after reaching the setpoint value.

Measurements in the selected points of the described processes, fig. 1, were used for calculating thermal, exergy and exergoeconomic variables. The CoolProp software used in all calculation of thermodynamic analysis [21]. Besides thermal measurements (temperature, pressure, and flow), electricity consumption was recorded. For every parameter, basic statistics were applied and the average value, median and standard deviation were calculated based on the following expressions [22]:

$$\bar{X} = \frac{1}{N}\sum_{i=1}^{N} X_i \tag{21}$$

$$\mu_X = \begin{cases} X_j, & \text{where is } j = (N+1)/2 \text{ and } N \text{ odd number} \\ \dfrac{X_j + X_{j+1}}{2}, & \text{where is } j = N/2 \text{ and } N \text{ even number} \end{cases} \tag{22}$$

$$\sigma_X = \left| \sqrt{\frac{1}{N}\sum_{i=1}^{N}\left(X_i - \bar{X}\right)^2} \right| \tag{23}$$

Statistical analysis of the measurement reveals that for both types of operation enough data was obtained, and that average values could be used for further analysis.

Besides these statistical values, tab. 2, gives the overview of values of the most important thermodynamic, exergy and exergoeconomic parameters of the overall system, for both types of operation.

Performance metrics based on energy (COP) during UFH operation varies around the mean value of 3.77 during the entire operating period, and maintains the trend of a constant value, fig. 3(a). Frequency distribution of experimental results is concentrated around this

mean value, since the standard deviation is 0.36 or 9.55%. Out of 690 values (N_{UFH} = 690), COP for 435 of them (63%) is within the interval of one standard deviation ([$\overline{COP}_{UHF} \pm \sigma_{UHF}$]) while the offset of the mean value to the median value is only 0.53%, tab. 2. A greater distance from the mean value was observed during the system start, when AWHP operated at full capacity and when condensing temperature reached 44.6 °C.

The operating and maintenance cost rate for each component was calculated as a levelized annual cost for a period of 15 years with the annual escalation rate of 6% and the rate of return of 12% using the real present operating and maintenance cost for 3650 working hours per year.

Table 2. Statistical values of selected thermodynamic, exergy and exergoeconomic parameters for the overall system

Parameters	Unit	Low temperature UFH					DHW heating				
		Average	Median	St.dev.	Max.	Min.	Average	Median	St.dev.	Max.	Min.
t_{11}	[°C]	3.41	4.00	1.33	5.00	-0.50	3.84	2.00	2.66	8.00	1.00
Δt_{lift}	[°C]	38.86	38.50	1.68	44.60	36.80	45.33	46.20	5.00	53.90	33.50
COP	[–]	3.77	3.75	0.36	4.80	3.02	3.51	3.32	0.48	4.71	3.01
$\dot{E}_{F,tot}$	[kW]	0.79	0.62	0.32	1.61	0.46	3.61	4.15	0.94	4.79	1.91
$\dot{E}_{P,tot}$	[kW]	0.14	0.11	0.06	0.29	0.08	0.56	0.63	0.30	0.93	0.15
$\dot{E}_{D,tot}$	[kW]	0.61	0.48	0.27	1.36	0.33	1.63	1.67	0.38	2.33	0.87
$\dot{E}_{L,tot}$	[kW]	0.04	0.04	0.01	0.07	0.03	1.42	1.64	0.36	1.90	0.88
ε_{tot}	[%]	18.09	17.50	3.35	27.51	10.85	14.29	14.21	5.31	22.35	7.72
$\dot{Z}_{tot}^{OM}$	[€/h]	0.06	0.06	0.00	0.06	0.06	0.06	0.06	0.00	0.06	0.06
$\dot{C}_{F,tot}$	[€/h]	0.05	0.04	0.02	0.09	0.03	0.13	0.15	0.03	0.18	0.07
$\dot{C}_{P,tot}$	[€/h]	0.11	0.09	0.02	0.15	0.09	0.19	0.20	0.03	0.23	0.12
$\dot{C}_{D,tot}$	[€/h]	0.04	0.03	0.02	0.08	0.02	0.06	0.06	0.01	0.09	0.03
r_{tot}	[–]	11.97	12.65	3.07	17.89	5.50	11.44	8.36	6.15	22.40	5.16

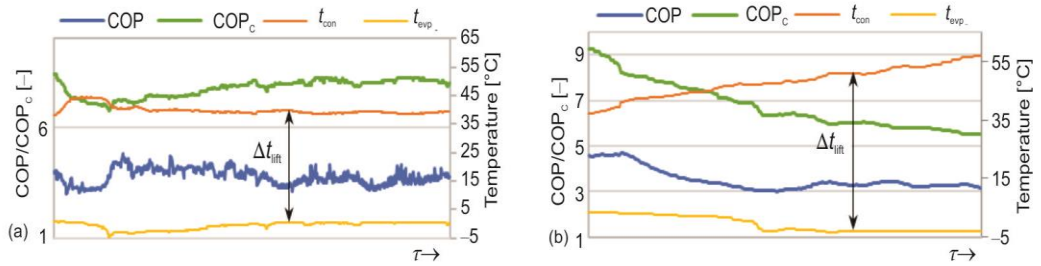

Figure 3. The energy-based efficiency measure of the overall heat pump system (real COP and Carnot COP) as a function of the difference between condensing and evaporating temperature; (a) low temperature UFH and (b) DHW heating

On the other hand, during DHW operation, fig. 3(b)., there was a significant drop of the COP value at the end ($COP_{DHW,min}$ = 3.01) compared to the system start when it had the maximum value ($COP_{DHW,max}$ = 4.71). The standard deviation of COP during this type of operation was higher compared to UHF operation and is 13.67%. Out of 197 measured values, 160 were within one standard deviation from the mean value ([$\overline{COP}_{DHW} \pm \sigma_{DHW}$]) thus giving the Gaussian distribution. The difference between the mean and the median value was slightly bigger and is around 5.4%.

The observed difference between the mean and the median value, during DHW operation can be seen by comparing figs. 3(a) and 3(b)., where in the first case the temperature difference between condensing and evaporating temperature is almost constant, fig. 3(a), while in the second case this difference is constantly increasing, fig. 3(b). These differences are directly followed with Carnot efficiency which increases with a decrease in Δt_{lift}, fig. 3(a), and vice versa, fig. 3(b). From the energy point of view, UFH operation of AWHP is 6.9% more efficient compared to DHW operation.

Exergy efficiency of the observed system experiences a slight decrease with a fuel exergy increase during UFH operation, fig. 4(a), as expected since higher values of fuel exergy are common for the AWHP start (the compressor and condenser efficiencies have minimum values). After adjusting the compressor output to real energy needs, fig. 2, exergy efficiency of the components and AWHP maintained constant values, fig. 4(a). Having in mind that during DHW operation AWHP capacity steadily increased, fig. 2(b)., fuel exergy replicated this trend. The system's exergy efficiency rose to the maximum value, and then decreased to the minimum, fig. 4(b). It is interesting that for fuel exergy of 3.9-4.1kW, when exergy efficiency reached the maximum value, at the same time AWHP output capacity reached its maximum value (based on the manufacturer catalogue) [23]. With a further increase in fuel exergy, irreversibilities in the compressor increased, which was followed by a drop in AWHP efficiency.

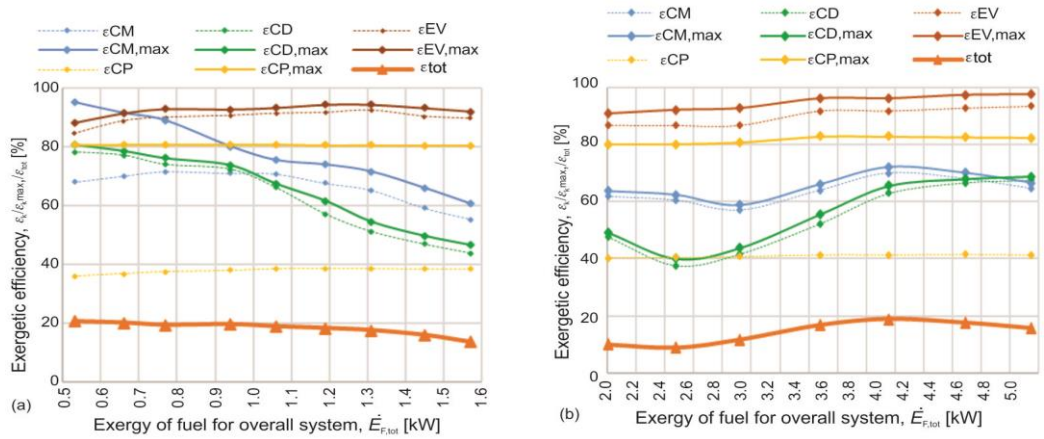

Figure 4. Recorded and maximum exergetic efficiency of the components and the system as a function of fuel exergy of the overall system; (a) low temperature UFH and (b) DHW heating

The application of advanced exergy analysis revealed that the circulating pump has the lowest exergy efficiency (cca 40%) which can be doubled, but since it has small absolute values, its impact on AWHP exergetic efficiency is minimal. For improving the overall system's exergetic efficiency it is far more important to increase exergetic efficiency of the compressor, condenser, and evaporator, which, on average, can be increased by 9.23%, 4.41%, and 2.72%, respectively, during UFH operation and 3.04%, 3.88%, and 5.22%, respectively, during DHW operation.

Figure 5(a) shows that the mean value of exergy efficiency during UHF operation (18.09%) is 21% larger than DHW operation (14.29%), which can lead to the conclusion that during this type of operation AWHP operates with more favourable operating conditions. Du-

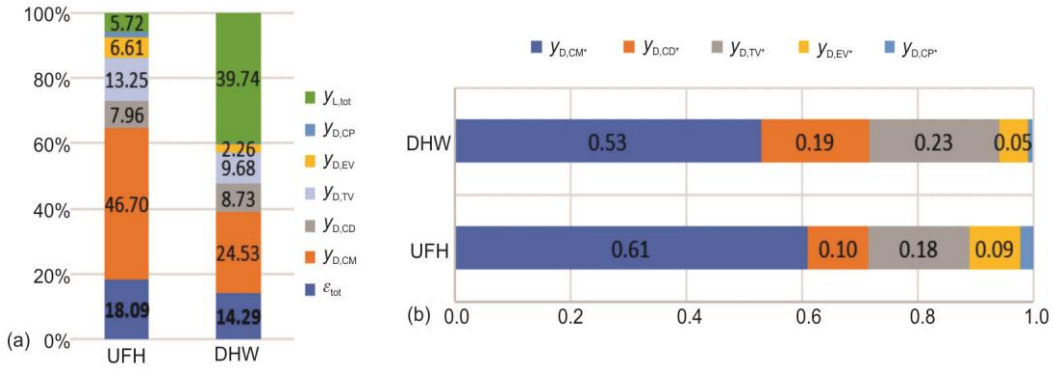

Figure 5. Comparison of exergy related parameters for UFH and DHW; (a) exergetic efficiency and (b) total exergy destruction ratios

ring UHF operation, the compressor has the biggest impact on reducing exergy efficiency with the exergy destruction coefficient of 46.7%, fig. 5(a). Although a relatively small amount of fuel exergy is required (0.79 kW), tab. 2, due to the component's irreversibility a fair amount of exergy destruction is generated (0.37 kW) out of which 51% (0.19 kW) represents unavoidable exergy destruction, fig. 6(a). On the other hand, during DHW operation, the influence of the compressor is twice smaller (24.53%), since with 3.61 kW of fuel exergy, a significantly smaller amount of exergy destruction is generated (0.85 kW), out of which 90% goes to the unavoidable part, fig. 7(a). This can be attributed to the fact that during certain time in UFH operation, the compressor operated under unfavourable conditions (operating at lower capacities). The dominant effect on the overall system exergy efficiency reduction is observed from the exergy loss coefficient during DHW (39.74%), due to heat exchange with the environment (heat losses). Since higher temperature levels were reached during this operation, fig. 2(b), this value is significant. The influence of the condenser and evaporator, for both operation regimes, is given in fig. 5(a), and ranges from 2.26 (6.61)%-8.73 (7.96)%, while the influence of the circulating pump can be neglected. The values of the total exergy destruction coefficients, fig. 5(b), confirm the previous statement regarding the exergy destruction in the compressor being dominant for both operating regimes with the values of 0.61 (UHF) and 0.53 (DHW). It should be noted that the influence of the throttling valve on exergy efficiency (decrease of 13.25% and 9.68%, fig. 5a.) can be lowered by replacing it with an expansion machine. Having in mind a rather expensive investment cost for such an expansion machine, this option is been addressed in this paper.

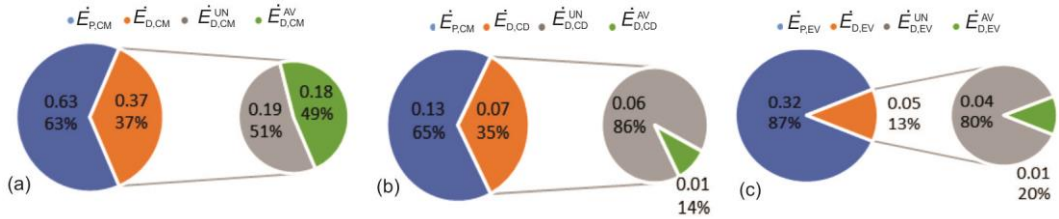

Figure 6. Fuel exergy decomposition and exergy destruction for three components during UHF operation; (a) compressor, (b) condenser, and (c) evaporator

By comparing the results presented in figs. 6(b) and 7(b), the ratio of exergy of products and exergy destruction is similar for both operating regimes, as well as the ratio of

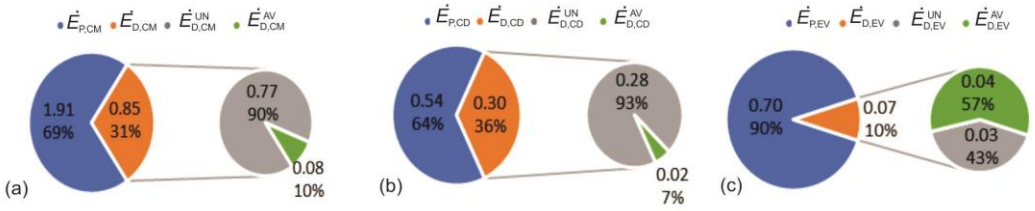

Figure 7. Fuel exergy decomposition and exergy destruction for three components during DHW operation; (a) compressor, (b) condenser, and (c) evaporator

avoidable and unavoidable exergy destruction, which further leads to the conclusion that the operating regime does not influence the condenser operation. On the other hand, although the same trends exist for the evaporator, there is a significant potential for improvement during DHW operation ($\dot{E}_{D,EV}^{AV}$ = 57%). The evaporator is probably the most important part of the heat pump since it represents the place where heat is recovered [24].

The biggest relative increase in average costs per unit of exergy between fuel and product, represented in the form of relative cost differences, is displayed by CP, fig. 8(a), with the values of 10.91 during UFH operation and 4.81 during DHW operation. The reason lies in the ratio of fuel and product exergy for this component. Yet, absolute values are rather small, and components CM, CD, EV are much more significant for increasing the overall system efficiency. Values of relative cost differences for both operating regimes are similar for components CD (0.57, 0.89) and EV (1.16, 1.06), fig 8(a), while for component CM this value is significantly higher during UFH operation (2.16) compared to DHW operation (0.58). The reason for the high value during UFH operation is in AWHP operating with small capacities, so the cost per unit of exergy for the same economic parameters is higher.

Thus, the general recommendation is to, first, set the AWHP to operate with near-optimal capacities and then reduce exergy of flows 1, 2, 5, 11, and 13, fig. 1(a), with the idea of increasing the individual component efficiency thus leading to an increase in the overall system efficiency.

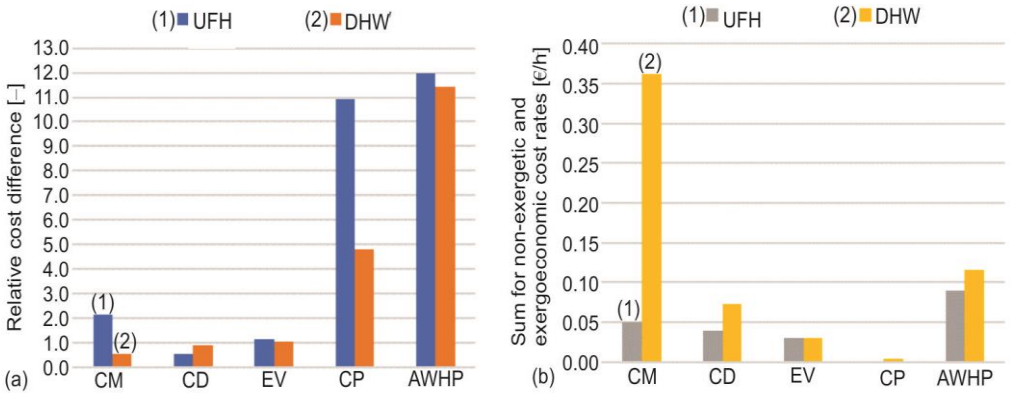

Figure 8. Comparison of exergoeconomic variables for UFH and DHW; (a) relative cost difference, (b) sum of non-exergetic and exergoeconomic cost rates

As stated before, non-exergetic costs are related only to operation and maintenance. The component with the largest total cost rates (the sum of non-exergetic and exergetic cost

rates) is CM, which should have the priority for improvements. The total cost rates for CM, during DHW operation, have the value of 0.36 EUR/h, fig. 8(b), due to high values of this component's fuel exergy. During UFH operation this value drops to 0.05 EUR per hours. The same applies for this exergoeconomic variable, as for the relative cost difference: the next components for improvements are CD and EV, fig. 8(b). The throttling valve as the component that serves the others and whose replacement with an expansion machine is not economically viable is not treated.

Conclusions

Scientific methods based on exergy can be used for energy system analysis equally at the component and system level. Results of conventional, energy analysis and advanced exergy analysis and exergoeconomic evaluation lead to the following conclusions for the described energy system (AWHP):

- From the energy analysis standpoint, it operates with satisfying performance for both operating regimes ($\overline{\mathrm{COP}}_{\mathrm{UHF}} = 3.77, \overline{\mathrm{COP}}_{\mathrm{DHW}} = 3.51$).
- Exergetic efficiency has a rather small value for both cases ($\bar{\varepsilon}_{\mathrm{UHF}} = 18.09\%, \bar{\varepsilon}_{\mathrm{DHW}} = 14.29\%$), with the largest influence during UHF operation attributed to irreversibilities in the compressor, and to irreversibilities in the compressor and exergy loss during DHW operation.
- The AWHP has high exergoeconomic costs of lost (destroyed) available work ($\bar{C}_{\mathrm{D,tot,UHF}} = 0.038$ €/h and $\bar{C}_{\mathrm{D,tot,DHW}} = 0.059$ €/h), which represents 76% of exergoeconomic cost for fuel during UHF operation and 45% during DHW operation.

These results show that AWHP is over-dimensioned for UHF operation as described but it has enough capacity for DHW operation. Destroyed work in the compressor has the greatest impact on reducing the overall system's exergetic efficiency with 46.7% during UFH operation and 24.53% during DHW operation. Exergy destruction of the other components contributes with 29.49% (UFH) and 21.44 (DHW). Exergy loss reduces exergetic efficiency by 5.72% (UFH) and 39.74% (DHW). High values of exergoeconomic cost for both operating regimes are present in flows 1-4 due to high costs of production and relatively small exergy levels.

Advanced exergy analysis shows that 51% of lost work in CM is unavoidable during UFH, and 90% is unavoidable during DHW operation, while the rest can be avoided by applying available state-of-the-art technologies.

To increase exergy/energy efficiency of AWHP it is of crucial importance to reduce internal irreversibilities of the compressor while operating with lower capacities, which reduces losses to the environment, and finally operates the system at the design/nominal operating conditions.

Analysis of individual components' exergetic efficiency and the overall system's exergetic efficiency reveals that the selection of the heat pump should be adjusted to end users, reducing the impact of the compressor's exergy destruction coefficient. Further, it is revealed that condensing temperature should be as low as possible, which is the same conclusion as the one derived from conventional energy analysis.

Acknowledgment

This research was financially supported by the Ministry of Education, Science and Technological Development of the Republic of Serbia (No. 451-03-68/2020-14200109).

Nomenclature

c – cost per unit exergy [€/GJ]
$\dot{C}$ – exergoeconomic cost rate [€/h]
e – specific exergy [kJkg^{-1}]
$\dot{E}$ – exergy flow rate [kW]
h – specific enthalpy [kJkg^{-1}]
$\dot{m}$ – mass flow rate [kgs^{-1}]
p – pressure [bar]
$\dot{Q}$ – heat transfer rate [kW]
r – relative cost difference [–]
s – specific entropy [kJkg^{-1}K^{-1}]
$\dot{S}$ – entropy rate [WK^{-1}]
t – temperature [°C]
T – absolute temperature [K]
$\dot{W}$ – power or work rate [kW]
X – current variable
y – exergy ratio [–]
$\dot{Z}$ – non-exergy cost rate [€h^{-1}]

Greek symbols

Δ – difference
ε – exergetic efficiency
μ – median
σ – standard deviation

Subscripts

C – Carnot
CD – condenser
CM – compressor
CP – circulation pump
cv – control volume
con – condensation
D – destruction
e – outlet stream
EU – end-user
EV – evaporator
evp – evaporation
F – fuel
gen – generated
i – inlet stream, current measure
j – stream
k – system component
lift – from condensation to evaporation
L – loss
max – maximal
min – minimal
N – total number of measures
P – product
q – heat transfer
sp – set point
TV – throttling valve
tot – overall system
w – generating power, water
X – current variable
0 – environment

Superscripts

AV – avoidable
CI – capital investment
max – maximal
OM – operating and maintenance
UN – unavoidable
PH – physical
* – total
¯ – arithmetic average

References

[1] Moran, M., Shapiro, H., *Fundamentals of Engineering Thermodynamics*, John Wiley & Sons Ltd., West Sussex, UK, 2006
[2] ***, https://www.iea.org/reports/tracking-buildings/heat-pumps
[3] ***, https://www.ehpa.org/market-data/market-overview/
[4] Morosuk, T., Tsatsaronis, G., Advanced Exergetic Evaluation of Refrigeration Machines Using Different Working Fluids, *Energy, 34* (2009), 12, pp. 2248-2258
[5] Dong, X., *et al*., Energy and Exergy Analysis of Solar Integrated Air Source Heat Pump for Radiant Floor Heating Without Water, *Energy and Buildings, 142* (2017), May, pp. 128-138
[6] Zhang, R., *et al*., A Novel Variable Refrigerant Flow (VRF) Heat Recovery System Model: Development and Validation, *Energy and Buildings, 168* (2018), June, pp. 399-412
[7] Qui, J., *et al*., Experimental Investigation of L-41b as Replacement for R410A in a Residential Air-Source Heat Pump Water Heater, *Energy and Buildings, 199* (2019), Sept., pp. 190-196
[8] Xu, S., *et al*., Experimental Study on R1234yf Heat Pump at Low Ambient Temperature Comparison with Other Refrigerants, *Thermal Science, 23* (2019), 6B, pp. 3877-3886
[9] Xu, W., *et al*., Feasibility and Performance Study on Hybrid Air Source Heat Pump System for Ultra-Low Energy Building in Severe Cold Region of China, *Renewable Energy, 146* (2020), Feb., pp. 2124-2133
[10] Ahamed, U. J., *et al*., A Review on Exergy Analysis of Vapor Compression Refrigeration System, *Renewable and Sustainable Energy Reviews, 15* (2011), 3, pp. 1593-1600
[11] Alshehri, F., *et al*., Techno-Economic Analysis of Ground and Air Source Heat Pumps in Hot Dry Climates, *Journal of Building Engineering, 26* (2019), Nov., 100825

[12] Wang, D., *et al*., Energy and Exergy Analysis of an Air-Source Heat Pump Water Heater System Using CO_2/R170 Mixture as an Azeotropy Refrigerant for Sustainable Development, *International Journal of Refrigeration, 106* (2019), Oct., pp. 628-638
[13] Byme, P., Ghoubali, R., Exergy Analysis of Heat Pumps for Simultaneous Heating and Cooling, *Applied Thermal Engineering, 149* (2019), Feb., pp. 414-424
[14] Su, W., *et al*., Performance Investigation on a Frost-Free Air Source Heat Pump System Employing Liquid Desiccant Dehumidification and Compressor-Assisted Regeneration Based on Exergy and Exergoeconomic Analysis, *Energy Conversion and Management, 183* (2019), Mar., pp. 167-181
[15] ***, https://www.scienceeurope.org/media/0vxhcyhu/se_exergy_brochure.pdf
[16] Bejan, A., *et al*., *Thermal Design and Optimization*, John Wiley & Sons, Inc., New York, USA, 1996
[17] Cuhla, O., *et al*., Heat Exchanger Applications in Wastewater Source Heat Pumps for Buildings: A Key Review, *Energy and Buildings, 104* (2015), Oct., pp. 215-232
[18] Mergenthaler, P., *et al*., Application of Exergoeconomic, Exergoenvironmental, and Advanced Exergy Analysis to Carbon Black Production, *Energy, 137* (2017), Oct., pp. 898-907
[19] Ebrahimi, M., *et al*., Conventional and Advanced Exergy Analysis of a Grid Connected Underwater Compressed Air Energy Storage Facility, *Applied Energy, 242* (2019), May, pp 1198-1208
[20] Kelly, S., Energy System Improvement Based on Endogenous and Exogenous Exergy Destruction, Ph. D. thesis, TU Berlin, Berlin, Germany, 2008
[21] ***, http://www.coolprop.org/index.html
[22] Bulatović, J., *Statistical Processing of Measurement Results* (in Serbian), Edvard Kardelj, Niš, Serbia, 1982
[23] ***, https://www.daikin.rs/sr_rs/products/ERLQ-CV3.table.html
[24] Nyers, A., *et al*., Dynamic Behavior of a Heat Pump Coaxial Evaporator Considering the Phase Border`S Impact on Convergence, *Facta Universitatis, Series: Mechanical Engineering, 16* (2018), 2, pp. 249-259

Paper submitted: May 29, 2020
Paper revised: July 14, 2020
Paper accepted: August 7, 2020